ADVANCED MATERIALS
www.advmat.de

Quinoline-Flanked Diketopyrrolopyrrole Copolymers Breaking through Electron Mobility over 6 $cm^2 V^{-1} s^{-1}$ in Flexible Thin Film Devices

*Zhenjie Ni, Huanli Dong, Hanlin Wang, Shang Ding, Ye Zou, Qiang Zhao, Yonggang Zhen, Feng Liu, Lang Jiang, and Wenping Hu**

Herein, the design and synthesis of novel π-extended quinoline-flanked diketopyrrolopyrrole (DPP) [abbreviated as QDPP] motifs and corresponding copolymers named PQDPP-T and PQDPP-2FT for high performing n-type organic field-effect transistors (OFETs) in flexible organic thin film devices are reported. Serving as DPP-flankers in backbones, quinoline is found to effectively tune copolymer optoelectric properties. Compared with TDPP and pyridine-flanked DPP (PyDPP) analogs, widened bandgaps and strengthened electron deficiency are achieved. Moreover, both hole and electron mobility are improved two orders of magnitude compared to those of PyDPP analogs (PPyDPP-T and PPyDPP-2FT). Notably, featuring an all-acceptor-incorporated backbone, PQDPP-2FT exhibits electron mobility of 6.04 $cm^2 V^{-1} s^{-1}$, among the highest value in OFETs fabricated on flexible substrates to date. Moreover, due to the widened bandgap and strengthened electron deficiency of PQDPP, n-channel on/off ratio over 10^5 with suppressed hole transport is first realized in the ambipolar DPP-based copolymers.

Dr. Z. J. Ni, Prof. H. L. Dong, H. L. Wang, Dr. Y. Zou, Q. Zhao, Prof. Y. G. Zhen, Prof. L. Jiang, Prof. W. P. Hu
Beijing National Laboratory for Molecular Sciences
Key Laboratory of Organic Solids
Institute of Chemistry
Chinese Academy of Sciences
Beijing 100190, P. R. China
E-mail: huwp@iccas.ac.cn, huwp@tju.edu.cn

Dr. Z. J. Ni, Prof. W. P. Hu
Tianjin Key Laboratory of Molecular Optoelectronic Sciences
Department of Chemistry
School of Science
Tianjin University, and Collaborative Innovation Center of Chemical Science and Engineering (Tianjin)
Tianjin 300072, P. R. China

Prof. H. L. Dong, S. Ding
Beijing Key Laboratory for Optical Materials and Photonic Devices
Department of Chemistry
Capital Normal University
Beijing 100048, P. R. China

H. L. Wang, Q. Zhao, Prof. Y. G. Zhen, Prof. L. Jiang
School of Chemistry and Chemical Engineering
University of Chinese Academy of Sciences
Beijing 100049, P. R. China

Prof. F. Liu
Department of Physics and Astronomy
Shanghai Jiaotong University
Shanghai 200240, P. R. China

The ORCID identification number(s) for the author(s) of this article can be found under https://doi.org/10.1002/adma.201704843.

DOI: 10.1002/adma.201704843

Over the past years, flexible devices have gained wide attention to satisfy the mechanical requirements of wearable electronics and flexible display.[1,2] As the key element for driving and logic operations, high mobility and solution-processable organic field-effect transistors (OFETs), especially with polymer channel layer, are of great interests to realize low-cost and high-performing flexible devices.[3–5] Among these polymers, diketopyrrolopyrrole (DPP) presents a most adopted unit in copolymer synthesis.[6,7] DPP's good planarity facilitates intermolecular interchain interactions and π-electron delocalization to enhance carrier transport. Moreover, due to its electron deficiency, copolymerization of DPP with donor units can potentially lead to ambipolar materials.[8–10]

To date, thiophene-flanked diketopyrrolopyrrole (TDPP)-based polymers have been extensively investigated.[4,5] Especially, TDPP copolymers with common thiophene-derived donors have exhibited remarkably high hole mobilities in past reports.[11,12] However, electron mobility of these materials is largely lag behind their hole mobilities, most probably due to relatively weak electron deficiency and insufficient lowest unoccupied molecular orbitals (LUMO) levels for electron injection and transport. To address this issue, substitution of electron donors with acceptors, such as benzothiazole (BTz),[13] difluorothiophene (2FT),[14] tetrafluorobenzene (TFB),[15] and 1,2-bis(3,4-difluorothiophen-2-yl)ethene (4FTVT)[16] were carried out. Unfortunately, copolymers derived from this protocol generally display balanced ambipolar transport by identical hole/electron mobilities and dominant *n*-transporting ones are rare.[17] Furthermore, adoption of TDPP in the backbone of copolymers usually leads to narrowed bandgap, thereby deteriorating their *n*-channel on/off ratio (less than 1000).[6] Besides acceptor substitution, another route features molecular modification on DPP flankers. Electron-withdrawing units, such as pyridine (Py),[14,18] thiazole (Tz),[19] and π-extended DPP core[20] are adopted to strengthen polymer electron deficiency. However, these attempts fail to give high electron mobility products. Moreover, a majority of high electron mobility DPP polymers are fabricated on rigid substrates, restricting their application under flexible conditions. Hence, the acquisition of n-type DPP copolymers that simultaneously accommodate high electron

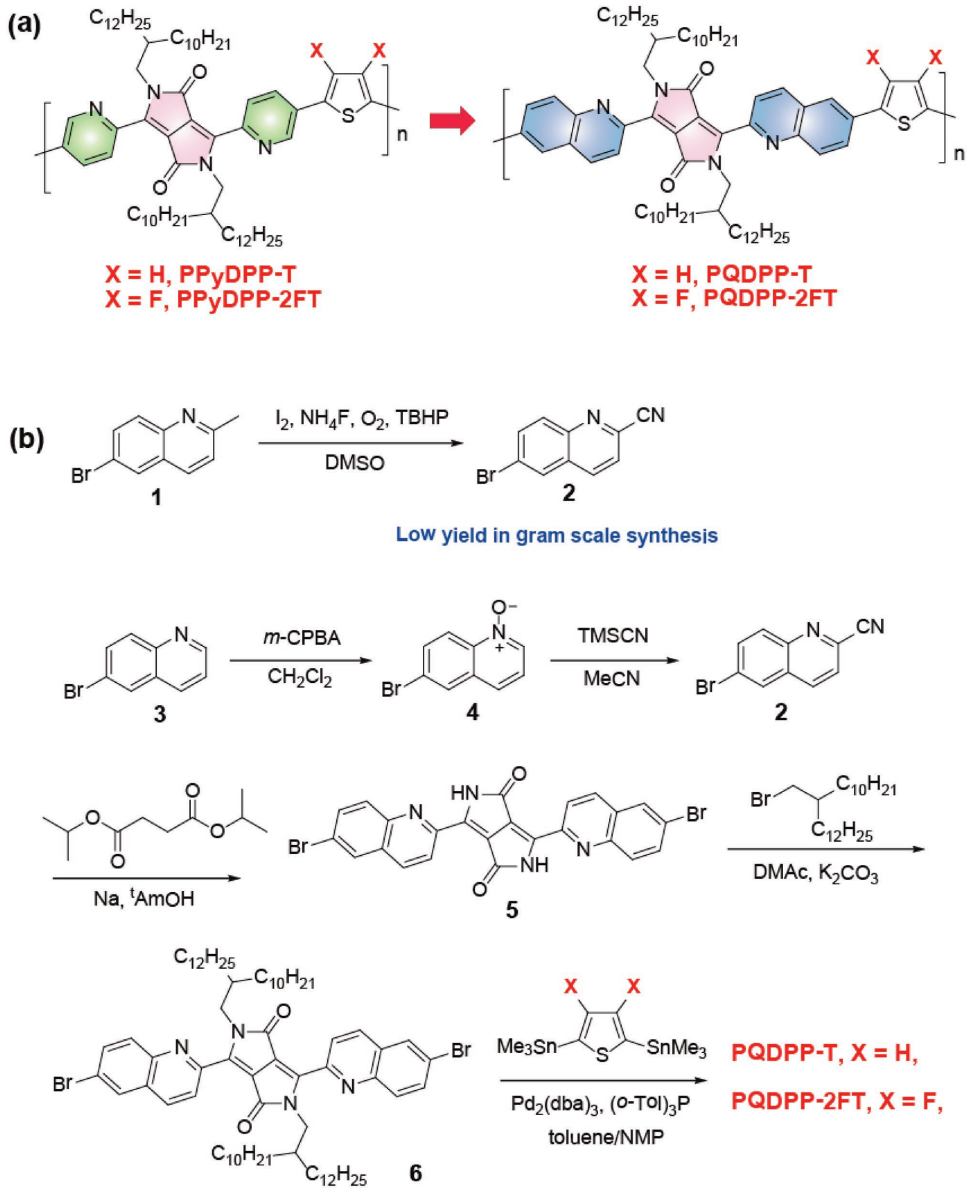

Figure 1. a) Molecular structures of the novel copolymers, **PPyDPP-T**, **PPyDPP-2FT**, **PQDPP-T**, and **PQDPP-2FT**. b) Synthetic procedures of the copolymers **PQDPP-T** and **PQDPP-2FT**.

mobility and on/off ratio on flexible substrates presents an urgent and demanding task.

Herein, to address aforementioned limitations, we report the design and synthesis of novel π-extended quinoline-flanked DPP (abbreviated as QDPP) motif and corresponding copolymers named **PQDPP-T** and **PQDPP-2FT** (**Figure 1**a) for high-performing n-type OFETs in flexible organic thin film devices. Serving as DPP flankers in backbones, quinoline is found to effectively tune copolymer optoelectric properties. Compared with TDPP and pyridine flanked DPP (PyDPP) analogs,[14,21] widened bandgaps and strengthened electron deficiency are achieved. Moreover, both hole and electron mobility are improved two orders of magnitude than those of PyDPP analogs (**PPyDPP-T** and **PPyDPP-2FT**). Notably, featuring an all-acceptor-incorporated backbone, **PQDPP-2FT** exhibits electron mobility of 6.04 $cm^2 V^{-1} s^{-1}$, among the highest value in OFETs fabricated on flexible substrates up to date. Moreover, due to the widened bandgap and strengthened electron deficiency of PQDPP, *n*-channel on/off ratio over 10^5 with suppressed hole transport is first realized in the ambipolar DPP-based copolymers.

The synthetic routes for **PQDPP-T** and **PQDPP-2FT** are depicted in Figure 1b. The important intermediate 6-bromoquinoline-2-carbonitrile **2** was synthesized via a one-step iodine-catalyzed ammoxidation of 6-bromo-2-methylquinoline **1** reported by Cheng.[22] However, the yield of **2** decreased obviously, when this procedure was carried out in gram scale. An alternative multistep protocol for compound **2** has been developed. The intermediate **2** was obtained from direct cyanation of 6-bromoquinoline *N*-oxide using a

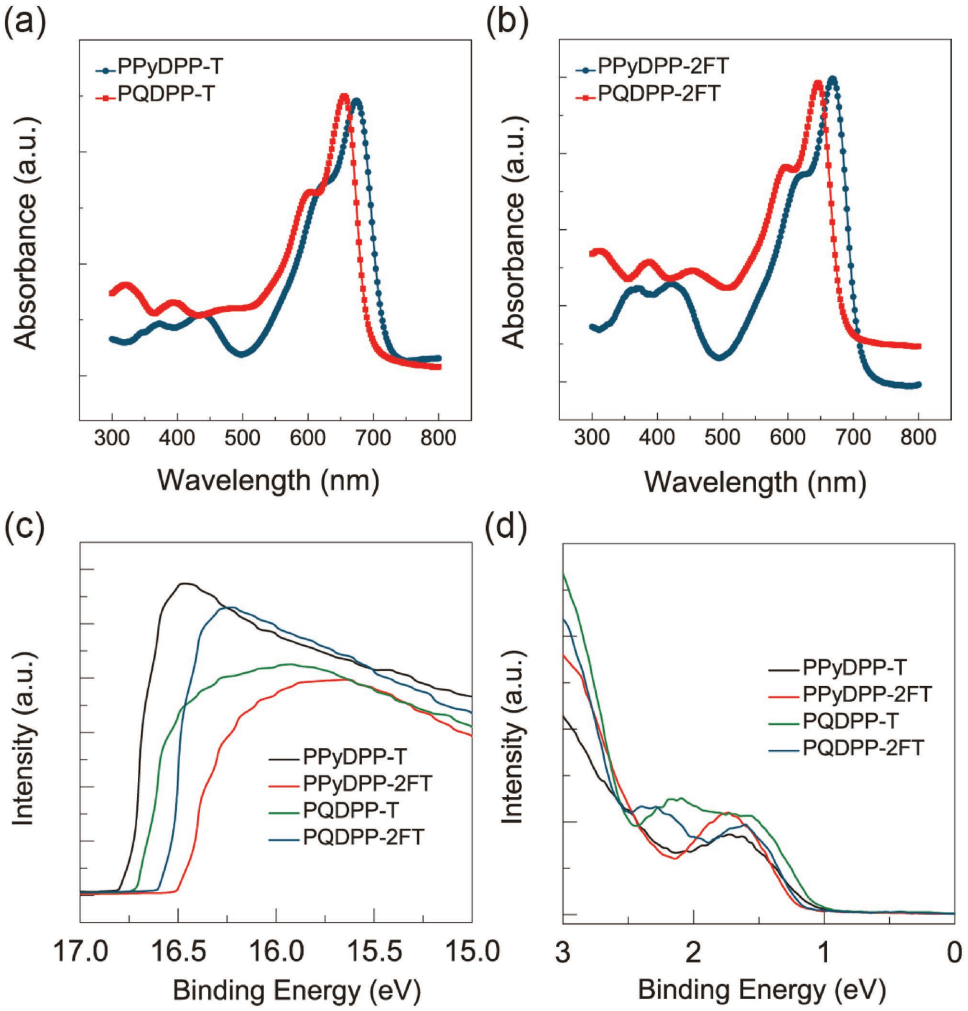

Figure 2. a,b) UV–vis–NIR absorption spectra of **PPyDPP-T** and **PQDPP-T**, **PPyDPP-2FT** and **PQDPP-2FT**. c) Secondary electron cutoff UPS spectra of polymers deposited on gold film. d) Valence band spectra.

less toxic trimethylsilyl cyanide as the cyano source.[23] Followed quinoline flanked DPP **5** was prepared by condensation reaction of **2** with diisopropyl succinate. The quinolone-flanked DPP monomer **6** was obtained after the *N*-alkylation of **5** with branched 2-decyltetradecyl chain, which ensures the sufficient solubility of the quinolone-flanked DPP polymers. Finally, polymers **PQDPP-T** and **PQDPP-2FT** were synthesized by a modified Stille polymerization of **6** with bis-stannylated thiophene or bis-stannylated difluorothiophene in high yield within only 10 min. For control experiment, reference polymers **PPyDPP-T** and **PPyDPP-2FT** were prepared by the similar procedure. The detailed synthetic procedures of polymers are described in the Supporting Information. Number-averaged molar mass (M_n) and dispersity (Đ) of 119.9 KDa and 1.84 for **PQDPP-T**, 67.4 KDa and 2.01 for **PQDPP-2FT**, 27.2 KDa and 2.92 for **PPyDPP-T**, and 20.2 KDa and 1.90 for **PPyDPP-2FT** were obtained after the removal of low molecular weight oligomers through Soxhlet extraction. Thermogravimetric analysis demonstrated that all polymers were thermally stable with a degradation temperature (T_d) higher than 350 °C (Figure S1, Supporting Information).

UV–vis spectroscopy was used to determine the bandgap of the polymers. Calculated from absorption onset in **Figure 2**a,b, bandgaps of **PPyDPP-T** and **PPyDPP-2FT** were 1.71 and 1.78 eV, respectively. Substitution of pyridine by quinoline flankers led to slightly widened bandgaps, which were 1.74 and 1.80 eV for **PQDPP-T** and **PQDPP-2FT**, respectively. The highest occupied molecular orbitals (HOMO) were measured by ultraviolet photoelectron spectroscopy (UPS) (Figure 2c,d) and summarized in **Table 1**. **PPyDPP-2FT** and **PQDPP-2FT**'s HOMO levels are –5.72 and –5.64 eV, respectively. Reduction of optical bandgaps from HOMO levels gives LUMO levels. Due to an all-acceptor alternating structure, their LUMO levels are –3.94 and –3.84 eV for **PPyDPP-2FT** and **PQDPP-2FT**, respectively, and notably lower than those of thiophene-flanked DPP polymers. Hence, enhanced electron transport over reported DPP polymers is highly anticipated. For comparison, density functional theory (DFT) calculation for methyl-substituted trimers were conducted by B3LYP/6-31G (d,p). The optimized structures

Table 1. Bandgaps and energy levels of the copolymers.[a)]

Polymer	E_g [eV]	HOMO [eV]	LUMO [eV]
PPyDPP-T	1.71	−5.33	−3.62
PPyDPP-2FT	1.78	−5.72	−3.94
PQDPP-T	1.74	−5.42	−3.68
PQDPP-2FT	1.80	−5.64	−3.84

[a)]Bandgaps of polymers were measured by absorption onset ($E_g = 1240/\lambda$) by UV–vis spectroscopy. HOMO levels were obtained by ultraviolet photoelectron spectroscopy. LUMO levels were calculated by subtraction of bandgaps from HOMO levels.

and frontier molecular orbitals of four trimers are displayed in Figure S2 (Supporting Information). Their HOMO and LUMO were well delocalized along their backbones. The DFT calculation showed that **PPyDPP-T**, **PPyDPP-2FT**, **PQDPP-T**, and **PQDPP-2FT** trimers' HOMO were −5.12, −5.23, −5.17, and −5.25 eV, respectively, and their LUMO levels were −3.09, −3.24, −3.05, and −3.15, respectively. Though simulation energetic levels of four trimers are different from UPS results, they share the identical tendency by: (i) Quinoline flankers delivered widened the polymer bandgaps. (ii) Deeper LUMO energy levels in **PPyDPP-2FT** and **PQDPP-2FT**, resulting from synergistic effect of electron-deficient pyridine/quinoline flankers and 3,4-difluorothiophene units.

The ambipolar transport properties of PPyDPP- and PQDPP-based copolymers were evaluated by OFET characterization. To facilitate electron channel stable in ambient atmosphere, OFETs were fabricated with a top-gated architecture on polyethylene terephthalate (PET) (**Figure 3**a,b). Polymer active layers were spin-coated from *o*-dichlorobenzene (*o*-DCB) solution on predefined gold contacts. Then, 900 nm polymethylmethacrylate (PMMA) served as dielectric[17] (C_i, 3.3 nF cm^{-2}) and 50 nm thermally-deposited aluminum was used as gate. Saturation mobility was extracted using I_{DS} square root dependence on gate voltage (V_G) under a V_{DS} of ±80 V. Overall, PQDPPs exhibit evidently higher hole and electron mobility than those of PPyDPPs by two orders of magnitude, as summarized in **Table 2**. Hole/electron mobilities of **PPyDPP-T** are rather low ranged from 10^{-4} to 10^{-3} cm^2 V^{-1} s^{-1} (Figure S3, Supporting Information). With the introduction of a strong electron-accepting unit, 2FT in the polymer backbone, **PPyDPP-2FT** showed enhanced electron mobility tenfold times higher than that of **PPyDPP-T**, up to 0.021 cm^2 V^{-1} s^{-1}. Meanwhile, its hole mobility is reduced

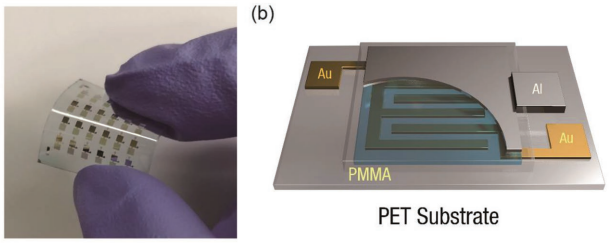

Figure 3. a) OFET array fabricated on flexible PET substrate. b) 3D schematic illustrating the top-gated OFET structure for the characterization of the copolymers.

to 10^{-4} cm^2 V^{-1} s^{-1}. This is probably due to the large hole injection barrier of 1.02 eV in **PPyDPP-2FT**/Au interface due to the low-lying HOMO level (−5.72 eV) of **PPyDPP-2FT**, making hole transport injection limited.

In contrast to PPyDPPs, **PQDPP-T** showed much improved and balanced ambipolar charge transport with hole and electron mobilities of 0.50 and 0.72 cm^2 V^{-1} s^{-1}, respectively (Figure S4, Supporting Information). Though **PQDPP-2FT**'s LUMO level (−3.84 eV) is 0.1 eV higher than PPyDPP-2FT (Table 1), an unexpectedly high electron mobility of 6.04 cm^2 V^{-1} s^{-1} is obtained (**Figure 4**). Similar to **PPyDPP-2FT**'s dominant electron transport property, **PQDPP-2FT** demonstrates an evidently suppressed hole channel with mobility of 0.21 cm^2 V^{-1} s^{-1}, giving a μ_e/μ_h ratio of 30. (Table 2). Contact resistance was acquired by the transfer-line method and calculated to be 20.4 kΩ cm for PQDPP-2FT and 117.4 kΩ cm for PQDPP-T, which is in good accordance with their LUMO level (Figure S5, Supporting Information). Note that reported TDPP polymers with a donor–acceptor or acceptor–acceptor backbone prototype are generally *p*- or ambipolar-transporting.[6,7] To our knowledge, **PQDPP-2FT** is one of the few DPP polymers demonstrating dominant *n*-channel features. These findings indicate that: (i) Quinoline flankers are more advantageous over pyridine or thiophene for highly efficient *n*-channel DPP-based polymers. (ii) 2FT presents a powerful electron accepting unit. Conjunction of 2FT unit with QDPP core enables an all-acceptor containing polymer backbone. Therefore, **PQDPP-2FT** possesses strong electron deficiency, potentially facilitating electron transport and *n*-channel formation.

Furthermore, a correlation between electron-channel onset voltage ($V_{e,\ onset}$) and LUMO level is uncovered. Among four polymers, **PPyDPP-2FT** shows the lowest $V_{e,onset}$ of 20 V (LUMO, −3.94 eV), while **PQDPP-T** and **PPyDPP-T** require high V_G (over 40 V) to turn-on electron channel (Table 2). This result imply a low-lying LUMO level is potentially beneficial for $V_{e,onset}$ reduction. Similar correlation between HOMO and hole-channel onset voltage is also found and shown in Table 2. Though a large electron injection barrier are to be expected between **PPyDPP-T** and **PQDPP-T**/Au interface (0.98 and 0.92 eV), output characterisitics at low V_{DS} region do not suggest similar conclusion (Figures S3 and S4, Supporting Information). Therefore, we postulate that high thin film quality and microstruture are other factors governing OFET performance.

Due to fused heterocycles (quinoline) in **PQDPP-2FT** backbone, its operation under various illumination conditions was investigated. Under 365 nm (6.22 mW cm^{-2}) and 550 nm (9.54 mW cm^{-2}) light exposure, **PQDPP-2FT** displays limited V_{Onset} shift (2–3 V) and I_{Off} increase by several ten-fold to 10^{-8} A and retains its original *n*-channel operation when illumination is ceased (Figure S6, Supporting Information), implying a tolerable photosensitivity for practical uses. Control experiments on **PQDPP-2FT** and **P(NDI2OD-T2)**[3] were also conducted for comparison. Under identical biasing conditions, **P(NDI2OD-T2)** exhibits μ_e of 0.50 cm^2 V^{-1} s^{-1}, on/off ratio of 10^3 and subthreshold swing of 7.5 V per decade, implying **PQDPP-2FT** a superior candidate as n-type OFETs (Figure S7, Supporting Information). Transport property of **PQDPP-2FT** is tested on 2 mm PET, its bending stress with a radius of 8 mm was conducted in Figure S8 (Supporting Information). After

Table 2. Thin film device characteristics of copolymers.[a)]

Polymer	μ_h ($cm^2 V^{-1} s^{-1}$)	$I_{on}/_{off}$ *p*-channel	$V_{h,\ onset}$ [V]	μ_e [$cm^2 V^{-1} s^{-1}$]	$I_{on}/_{off}$ *n*-channel	$V_{e,\ onset}$ [V]
PPyDPP-T	$5–8 \times 10^{-4}$	10^2	−38.0	$2–4 \times 10^{-3}$	10^2	37.5
PPyDPP-2FT	$1–3 \times 10^{-4}$	10	−59.0	0.015–0.021	10^3	20.0
PQDPP-T	0.28–0.50	10^3	−35.5	0.51–0.72	10^3	45.8
PQDPP-2FT	0.13–0.21	10^3	−47.7	4.25–6.04	10^5	35.0

[a)]OFETs were characterized within a V_G range from 0 to ±90 V and a V_{DS} of ±80 V.

200 times bending, it nearly retained its *n*-channel transfer curve unchanged.

We proceed to study thin film crystallization with grazing-incidence X-ray diffraction (GIXD) (**Figure 5**). Both PPyDPPs and PQDPPs exhibit strong crystallization feature. In out-of-plane orientation, both PPyDPPs and PQDPPs evidently display a succession of five (*h*00) peaks, implying an ordered lamellar packing in thin film state. Moreover, (010) diffraction peaks were also present in out-of-plane direction, indicating a mixed orientation of face-on and edge-on. π–π stacking distance was calculated using their in-plane (010) peaks. Especially, shorter in-plane π–π stacking distance was observed in PQDPPs, which was 3.49 and 3.45 Å for **PQDPP-T** and **PQDPP-2FT**, respectively. By contrast, **PPyDPP-T** and **PPyDPP-2FT** possess a value of 3.60 and 3.53 Å. This observation is in good agreement with close π–π spacing effectively promotes charge transport by reducing interchain charge hopping barrier and leads to high mobilities. Crystal coherence length is a parameter quantifying the polymer crystalline order range, which is calculated using the Scherrer equation.[24] Polymers with 2FT segment display higher range of crystalline order. In-plane (010) coherence lengths for **PPyDPP-T**, **PPyDPP-2FT**, **PQDPP-T**, and **PQDPP-2FT** were 32.2, 41.8, 29.4, and 65.2 Å, respectively. These results clearly indicate: (i) With π-extended conjugation length, quinoline flankers deliver stronger intermolecular interactions than pyridine in DPP polymer backbone. (ii) 2FT unit render denser polymer packing, as well as crystalline structure with greater range than thiophene unit. This is probably due to the formation of hydrogen bonding between fluorine atoms on 2FT and aromatic hydrogen atoms on quinoline/pyridine flankers. Such an intramolecular interaction can enhance the planarity of polymer backbone to facilitate efficient interchain charge transport. Besides above findings, all polymers except **PQDPP-2FT** exhibit a more pronounced (010) diffraction pattern in out-of-plane direction than in-plane. In other words, these three polymers are inclined to adopt a preferential face-on

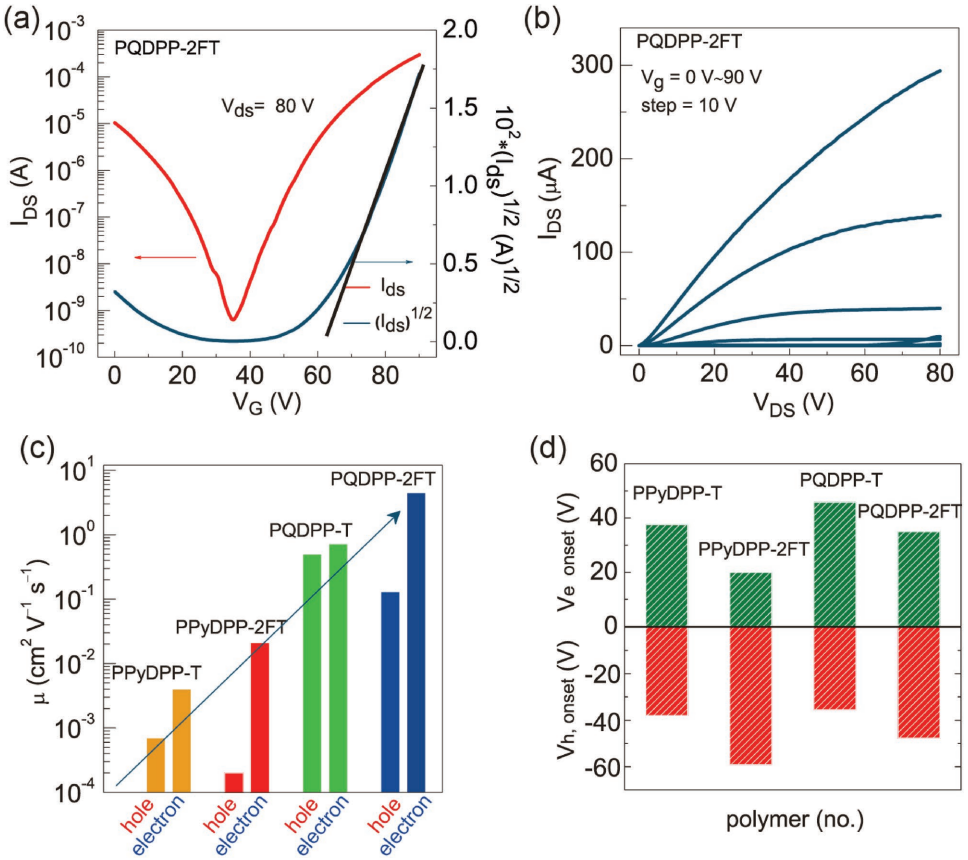

Figure 4. a) n-type transfer characteristics of **PQDPP-2FT**. b) n-type output characteristics of **PQDPP-2FT**. c) A summary of ambipolar mobilities of the four copolymers. d) $V_{e,\ onset}$ and $V_{h,\ onset}$ of the four copolymers.

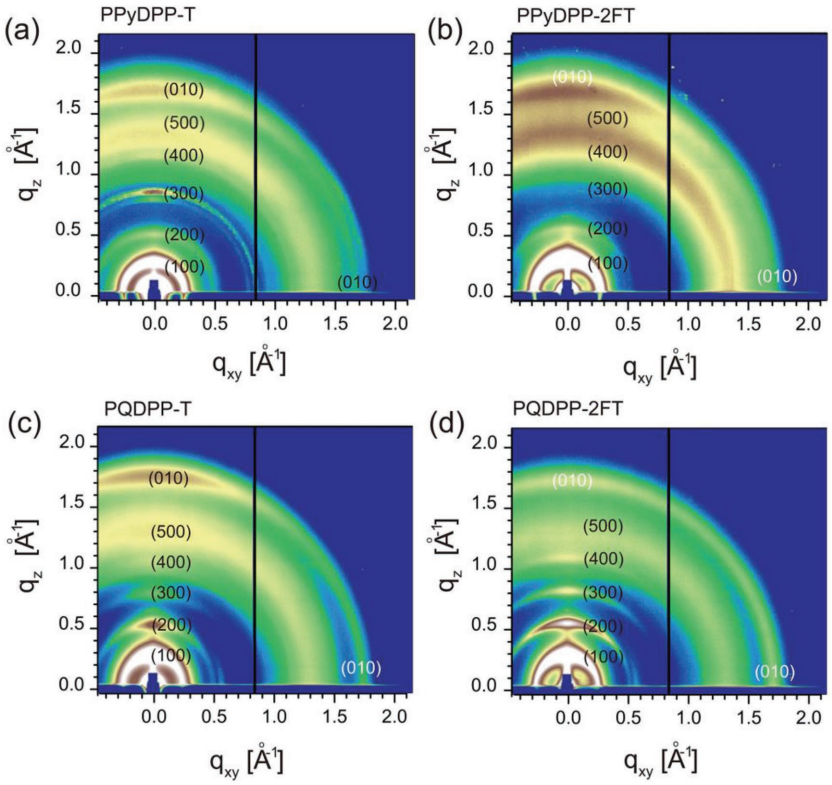

Figure 5. 2D-GIXD diffraction images of a) **PPyDPP-T**, b) **PPyDPP-2FT**, c) **PQDPP-T**, and d) **PQDPP-2FT** films.

packing in thin film. By contrast, this feature is less significant in the case of **PQDPP-2FT**. Edge-on rather than face-on packing is reported to be beneficial for highly efficient charge transport (in horizontal direction from source to drain) in OFETs, which accounts for the superior electron mobility in **PQDPP-2FT**. Thin film morphology was studied by atomic-force microscopy in Figure S9 (Supporting Information). **PPyDPP-2FT**, **PQDPP-T**, and **PQDPP-2FT** showed smooth surfaces with root-square-mean roughness below 1 nm. **PPyDPP-T**'s surface is notably uneven (2.71 nm).

In conclusion, a quinoline-flanked DPP acceptor was designed and synthesized efficiently. Copolymerization with thiophene/difluorothiophene afforded two copolymers **PQDPP-T** and **PQDPP-2FT** with widened bandgaps and strengthened electron deficiency compare to their PyDPP and TDPP analogs. Moreover, in this manuscript, we show: (i) As indicated by X-ray diffraction, PQDPPs display enhanced intermolecular interaction by shortened π–π stacking distances, which is advantageous for achieving high-performing polymers. (ii) OFET characterization and ultraviolet photoelectron spectroscopy uncover a preferential electron transport rather than hole and deep-lying LUMO in PQDPP. The all-acceptor containing copolymer **PQDPP-2FT** exhibits an electron mobility over 6.00 cm^2 V^{-1} s^{-1} with on/off ratio over 10^5, which is among the highest value in OFETs fabricated on flexible substrates to date. Our results demonstrate that QDPP is a superb building unit for high-performance OFET polymers.

Experimental Section

Synthesis of PQDPP-2FT: Under an argon atmosphere, (3,4-difluorothiophene-2,5-diyl) bis(trimethylstannane) (45.7 mg, 0.10 mmol), 3,6-bis(6-bromoquinolin-2-yl)-2,5-bis(2-decyltetradecyl)pyrrolo[3,4-*c*]pyrrole-1,4(2*H*,5*H*)-dione (122.1 mg, 0.10 mmol), $Pd_2(dba)_3$ (2.7 mg, 0.003 mmol, 3 mol %), and (*o*-Tol)$_3$P (2.7 mg, 0.009 mmol, 9 mol %) were dissolved in degassed toluene (3 mL) and NMP (0.6 mL) in a Schlenk tube. The reaction was stirred at 110 °C for 10 min, followed by addition of 2-bromothiophene (0.3 mL) to react with the trimethylstannyl end group. The mixture was further stirred at 100 °C for 1 h. After cooling to room temperature, the mixture was precipitated into chilled methanol (20 mL). Then the crude polymer was collected by filtration and purified by Soxhlet extraction with acetone, hexane and the remaining product was dissolved with refluxing 1,1,2,2-tetrachloroethane. The tetrachloroethane solution was then concentrated by evaporation and precipitated into methanol, dried over vacuum. Finally, the desired polymer was obtained. 90% yield; GPC(1,2-dichlorobenzene, 120 °C): M_n = 67.4 KDa, M_w = 135.8 KDa, Đ = 2.01; Anal. Calcd. for $C_{76}H_{108}F_2N_4O_2S$, C, 77.37; H, 9.23; N, 4.75; Found: C, 77.20; H, 9.20; N, 4.49.

Device Fabrication: A top gate, bottom contact configuration was used to evaluate the polymer semiconductors. 200 µm thick PET substrates were rinsed with deionized water, ethanol, acetone, then dried by nitrogen before device fabrication. Next, 20 nm gold interdigitated fingers (channel width 4500 µm, channel length 90 µm) were deposited by thermal evaporation. All polymers were dissolved in 1,2-dichlorobenzene (*o*-DCB) with a concentration of 4 mg mL^{-1}. The polymer solution was spin-coated on PET at a speed of 1800 rpm and dried at 150 °C for 10 min on a hotplate. PMMA dissolved in *n*-butyl acetate (60 mg mL^{-1}) served as the dielectric and dried at 90 °C for 30 min. To complete the fabrication, 100 nm thick aluminum was thermally deposited through shadow mask as gate contact. OFET characteristics were carried out in ambient using a Keithley 4200 semiconductor characterization system.

Supporting Information

Supporting Information is available from the Wiley Online Library or from the author.

Acknowledgements

Z.J.N., H.L.D., H.L.W., and S.D. contributed equally to this work. The authors thank Dr. Yang Li and Dr. Yanfeng Dang for the DFT calculations. This work was supported financially by the Ministry of Science and Technology of China (2016YFB0401100, 2017YFA0204503, 2013CB933403, and 2013CB933504), the National Natural Science Foundation of China (51633006, 51733004, 91433115, 91222203, 91233205, 51303185, and 21473222), and the Chinese Academy of Sciences (XDB12030300).

Conflict of Interest

The authors declare no conflict of interest.

Keywords

charge transport, conjugated copolymers, electron mobility, flexible devices

Received: August 24, 2017
Revised: December 12, 2017
Published online:

[1] M. L. Hammock, A. Chortos, B. C.-K. Tee, J. B.-H. Tok, Z. Bao, *Adv. Mater.* **2013**, *25*, 5997.
[2] A. Chortos, Z. Bao, *Mater. Today* **2014**, *17*, 321.
[3] H. Yan, Z. Chen, Y. Zheng, C. Newman, J. R. Quinn, F. Dötz, M. Kastler, A. Facchetti, *Nature* **2009**, *457*, 679.
[4] J. Zaumseil, H. Sirringhaus, *Chem. Rev.* **2007**, *107*, 1296.
[5] C. Wang, H. Dong, W. Hu, Y. Liu, D. Zhu, *Chem. Rev.* **2012**, *112*, 2208.
[6] C. B. Nielsen, M. Turbiez, I. McCulloch, *Adv. Mater.* **2013**, *25*, 1859.
[7] Z. Yi, S. Wang, Y. Liu, *Adv. Mater.* **2015**, *27*, 3589.
[8] Y. Zhao, Y. Guo, Y. Liu, *Adv. Mater.* **2013**, *25*, 5372.
[9] A. J. Kronemeijer, E. Gili, M. Shahid, J. Rivnay, A. Salleo, M. Heeney, H. Sirringhaus, *Adv. Mater.* **2012**, *24*, 1558.
[10] J. T. Quinn, J. Zhu, X. Li, J. Wang, Y. Li, *J. Mater. Chem. C.* **2017**, *5*, 8654.
[11] J. Li, Y. Zhao, H. S. Tan, Y. Guo, C.-A. Di, G. Yu, Y. Liu, M. Lin, S. H. Lim, Y. Zhou, *Sci. Rep.* **2012**, *2*, 754.
[12] I. Kang, H.-J Yun, D. S. Chung, S.-K. Kwon, Y.-H. Kim, *J. Am. Chem. Soc.* **2013**, *135*, 14896.
[13] P. Sonar, S. P. Singh, Y. Li, M. S. Soh, A. Dodabalapur, *Adv. Mater.* **2010**, *22*, 5409.
[14] C. J. Mueller, C. R. Singh, M. Fried, S. Huettner, M. Thelakkat, *Adv. Funct. Mater.* **2015**, *25*, 2725.
[15] J. H. Park, E. H. Jung, J. W. Jung, W. H. Jo, *Adv. Mater.* **2013**, *25*, 2583.
[16] Y. Gao, X. Zhang, H. Tian, J. Zhang, D. Yan, Y. Geng, F. Wang, *Adv. Mater.* **2015**, *27*, 6753.
[17] H. J. Yun, S. J. Kang, Y. Xu, S. O. Kim, Y. H. Kim, Y. Y. Noh, S. K. Kwon, *Adv. Mater.* **2014**, *26*, 7300.
[18] B. Sun, W. Hong, Z. Yan, H. Aziz, Y. Li, *Adv. Mater.* **2014**, *26*, 2636.
[19] Z. Yuan, B. Fu, S. Thomas, S. Zhang, G. DeLuca, R. Chang, L. Lopez, C. Fares, G. Zhang, J.-L. Bredas, *Chem. Mater.* **2016**, *28*, 6045.
[20] H. Bronstein, Z. Chen, R. S. Ashraf, W. Zhang, J. Du, J. R. Durrant, P. S. Tuladhar, K. Song, S. E. Watkins, Y. Geerts, *J. Am. Chem. Soc.* **2011**, *133*, 3272.
[21] J. C. Bijleveld, A. P. Zoombelt, S. G. Mathijssen, M. M. Wienk, M. Turbiez, D. M. de Leeuw, R. A. Janssen, *J. Am. Chem. Soc.* **2009**, *131*, 16616.
[22] S. Guo, G. Wan, S. Sun, Y. Jiang, J.-T. Yu, J. Cheng, *Chem. Commun.* **2015**, *51*, 5085.
[23] A. Miyashita, T. Kawashima, C. Lijima, T. Higashino, *Heterocycles* **1992**, *33*, 211.
[24] J. Rivnay, S. C. Mannsfeld, C. E. Miller, A. Salleo, M. F. Toney, *Chem. Rev.* **2012**, *112*, 5488.

